JCTC Journal of Chemical Theory and Computation

ARTICLE

pubs.acs.org/JCTC

Combined Metadynamics and Umbrella Sampling Method for the Calculation of Ion Permeation Free Energy Profiles

Yong Zhang† and Gregory A. Voth*

Department of Chemistry, James Franck Institute, Institute for Biophysical Dynamics, and Computation Institute, University of Chicago, 5735 South Ellis Avenue, Chicago, Illinois 60637, United States

ABSTRACT: Free energy calculations are one of the most useful methods for the study of ion transport mechanisms through confined spaces such as protein ion channels. Their reliability depends on a correctly defined reaction coordinate (RC). A straight line is usually not a proper RC for such complicated processes, so in this work a combined metadynamics/umbrella sampling (MTD/US) method is proposed. In the combined method, the ion transport pathway is first identified by the MTD method, and then the free energy profile or potential of mean force (PMF) along the path is calculated using umbrella sampling. This combined method avoids the discontinuity problem often associated with normal umbrella sampling calculations that assume a straight line RC, and it provides a more physically accurate potential of mean force for such processes. The method is demonstrated for the proton transport process through the protein channel of aquaporin-1.

I. INTRODUCTION

Ion channels are a large class of proteins that regulate ion flow across the cell membrane. Nearly all cells depend on the proper functioning of these ion channels to transfer ions in and out of the cell. This class of proteins has been widely studied using various experimental techniques (see, e.g., refs 1−5) as well as theoretical calculations (see, e.g., refs 6−9).

Free energy calculations are one of the most important techniques in theoretical and computational chemistry and have been proven to be a powerful tool to study biological systems.[10] The calculated free energy profile along the channel described by a certain reaction coordinate (RC), i.e., the potential of mean force (PMF), contains essential information about the ion transport process and provides detailed insight into the ion transport mechanism.[11−17]

In general, to perform such calculations, the channel is aligned along one axis of the simulation system (usually the Z-axis) and the coordinate component along this axis is used as the RC. This is a convenient setup, but, as shown below, it may provide a calculated PMF that differs significantly from the one along a more realistic and more complicated RC and consequently gives misleading information about the ion transport process.

As an example, we calculated the PMF of a classical hydronium with no Grotthuss proton shuttling transported through a kinked carbon nanotube model, as shown in Figure 1. The classical hydronium has a partial charge −0.5 e on the oxygen atom and +0.5 e on each of the three hydrogen atoms. The tube has a pore of 8 Å in diameter. All of the carbon atoms are fixed in space, as was done in previous studies, and should not affect the results.[18] The carbon atoms interact with water oxygens through a Lennard-Jones potential with $\varepsilon = 0.128\,95$ kcal/mol and $\sigma = 3.2752$ Å. This setup allows a single water wire to form in the aperture.[19]

The PMFs were obtained along the reaction coordinate (Z-coordinate of the hydronium oxygen) using umbrella sampling (US) for different orientations of the same carbon tube, as shown in Figure 1. For this simple model, it is reasonable to believe that the hydronium transports along the kinked tube central axis. The PMF associated with the real hydronium transport pathway was thus also calculated and shown in Figure 1. As expected, the PMF curves for the two tube orientations using the Z-coordinate as reaction coordinate are different from the correct one, demonstrating that using the Z-coordinate as the reaction coordinate fails to properly describe the kink and the change in channel radius (due to the kink) even for such a simple model.

Ion channel proteins consist of amino acids and are heterogeneous in nature. The local environment in the channels is much more complicated than the carbon tube model described above. The PMF calculated assuming a straight line RC may describe the ion transport processes improperly and thus yield a misleading description of the underlying biological processes. Here, we propose a combined metadynamics (MTD) and US method, in which the ion transport pathway is first identified using the MTD method and then the US calculation is carried out along the pathway to obtain the PMF along a more physically reasonable ion transport RC.

The metadynamics method and the combined MTD/US method are briefly described in the next section, and the combined method is demonstrated in more detail in section III on a protein channel. Discussion and concluding remarks are then given in the last section.

II. METHODS AND SIMULATION DETAILS

Metadynamics[20−23] is a free energy method that is based on a biasing of the potential surface and is similar to umbrella sampling in this sense. But, in contrast to umbrella sampling, the bias or "hills" are dynamically placed on top of the underlying potential energy landscape and discourages the system from visiting the same points in the configurational space. The hill can

Received: February 10, 2011
Published: June 02, 2011

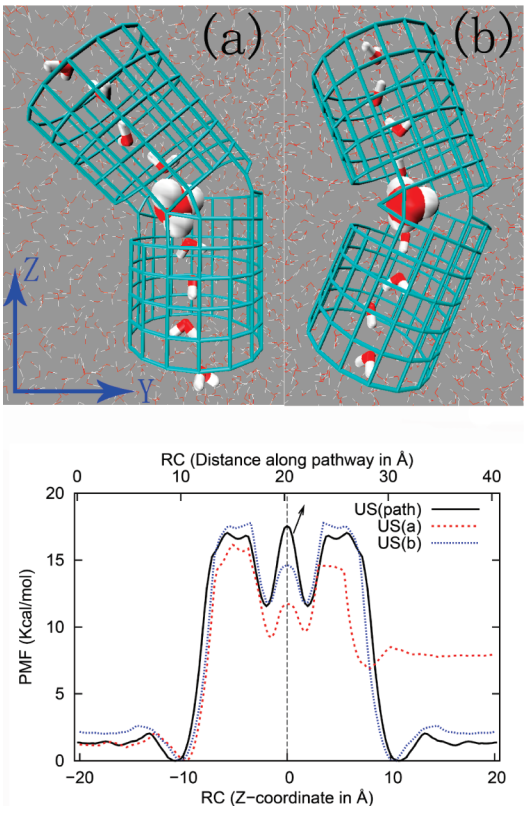

Figure 1. (Upper panels) Carbon tube model with a single water wire formed in the pore. The carbon atoms are fixed in space during the simulation and interact with water oxygen atoms through a van der Waals potential. (Lower panel) Calculated PMFs using the *Z*-coordinate as the reaction coordinate for different orientations (US(a), dotted line, and US(b), short dashed line, respectively) of the tube in space. The PMF calculated along the real ion transport pathway is also shown for comparison (US(path), solid line, up axis) and aligned at $Z = 0$ Å with the other two indicated by a dashed line. The statistical error was estimated to be ±0.2 kcal/mol or smaller. The difference in the calculated PMF profiles clearly demonstrates in this simple case that using a straight line along the *Z*-coordinate fails to properly describe the kink and radius change of the channel.

have any form, but a Gaussian potential is usually used:

$$V_{\text{bias}}(s,t) = \sum_{t_i} H \exp\left(-\frac{|s - s(t_i)|^2}{2w^2}\right) \quad (1)$$

where H is the height of the hill, w is the width, t is time, and s is the collective variable (CV) or RC. The hills are added at a time interval of δt. With the accumulation of hills, the local potential energy well is flattened and the system escapes the initial minimum over the lowest barrier. When applied properly, the MTD method not only accelerates the sampling of configuration space but also maps out the free energy surface or the potential of mean force as the negative of the sum of all the bias hills, $-V_{\text{bias}}(s,t)$.[20] The accuracy of the calculated PMF from MTD simulation depends on the parameters H, w, and δt, which in turn depend on the system properties. The selection of these parameters is not trivial[24] although successful applications have been reported.[25−30] The other issue that limits the application of the MTD method is a convergence problem caused by the lack of a straightforward way to determine at which point a MTD simulation should stop, and this causes error in the final PMF.[25,31−35] The well-tempered MTD method has solved this problem theoretically.[36] However, its successful application requires knowledge about the PMF of interest which is generally not known beforehand. Improperly chosen parameters may thus make the MTD PMF calculation inefficient or result in large errors.

Since MTD is able to find the next lowest barrier, it is also used as a path sampling method.[37,38] In the present work, instead of generating the PMF using MTD directly, we use it to find the ion transport pathway through an ion channel protein. Once the pathway is identified, the PMF along it can then be rigorously calculated using umbrella sampling. This combined MTD/US approach provides a powerful means to determine a complicated ion transport RC and then calculate a more physically meaningful PMF for the ion transport along that RC. The convergence problem sometimes associated with the MTD method for calculating the PMF is avoided.

For an arbitrarily curved pathway, instead of using the weighted histogram analysis method (WHAM),[39] the PMF or the free energy difference from the starting point can be calculated as[40,41]

$$F(s(\alpha)) - F(s(0)) = \int_0^\alpha d\alpha' \sum_{i=1}^{N} \frac{ds_i(\alpha')}{d\alpha'} \frac{\partial F(s(\alpha'))}{\partial s_i} \quad (2)$$

where $\alpha \in [0,1]$ is the parameter used to parametrize the path and the sum in the integral is over N RCs or CVs ($N = 1$ in the present work). The mean force can be calculated for each window by

$$\frac{\partial F(s)}{\partial s_j} \approx \frac{k}{T}\int_0^T dt\ (s_j - s_j(x(t))) \quad (3)$$

where k is the force constant in umbrella sampling, T is the simulation time, s_j is the equilibration value of the reaction coordinate, and $s_j(x(t))$ is its instantaneous value.

All simulations in this work were carried out at 308 K in the canonical ensemble (constant *NVT*) using DL_POLY package[42] or its modified version (see below) with the Amber force field.[43] The Nose−Hoover thermostat was used with relaxation time 0.5 ps. A MD integration time step of 1.0 fs was used, and the electrostatics were calculated by the smooth particle mesh Ewald method with a real space cutoff of 9.5 Å. The PLUMED package[44] was interfaced with DL_POLY for the MTD calculations.

III. RESULTS

The combined MTD/US method is demonstrated here for the protein channel aquaporin-1 (AQP1), which is a relatively simple channel protein but is more complicated than the carbon nanotube model discussed earlier. The exact ion transport pathway through AQP1 is not known. AQP1 is a channel protein that conducts water but effectively blocks protons and other positively charged ions through a high free energy barrier to ion permeation. Its selectivity mechanism has been extensively studied using various methods including free energy calculations.[1,11,16,45−51]

The PMF associated with proton transport through the AQP1 channel was calculated using the MTD/US method described above. The proton was treated either as a classical hydronium model or by using the multistate empirical valence bond (MS-EVB) model[52,53] that includes the full physics of Grotthuss proton shuttling and charge defect delocalization. The initial configuration containing the protein monomer and solvation

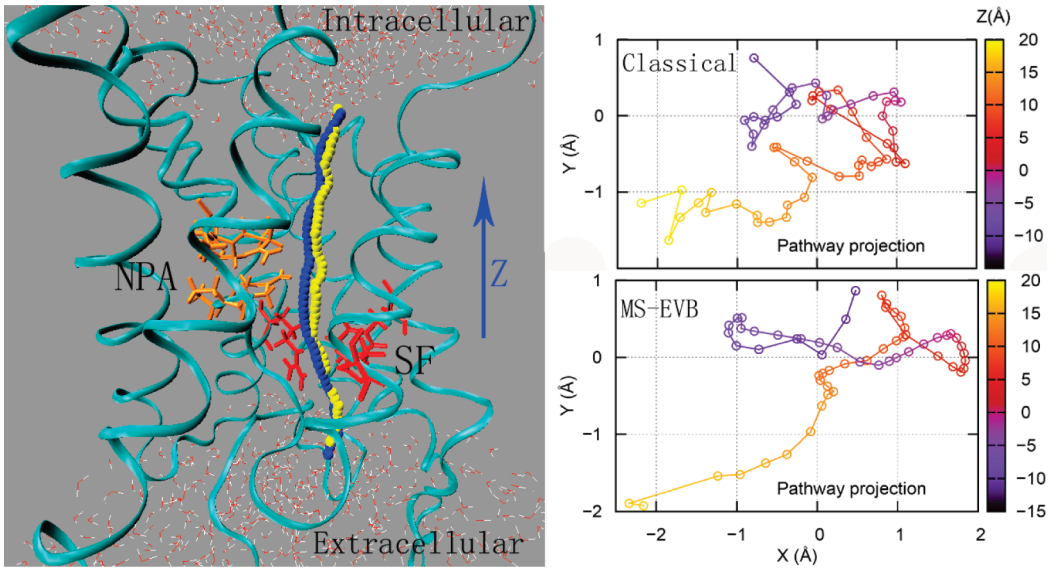

Figure 2. (Left) Structure of AQP1. The proton transport pathways identified by the metadynamics method are shown as yellow points for the classical hydronium model case and blue points for the excess proton described by the MS-EVB model. The NPA motif and the SF region, which form the two barriers for the proton transport, are shown in orange and red, respectively. (Right) Projection of the identified pathways onto the $X-Y$ plane with the Z-coordinate indicated by color. The pathways crossed > 3 Å in the X-direction and > 2 Å in the Y-direction. The pathways are twisted and clearly deviate from a straight line along the Z-coordinate, which would simply be a dot in the $X-Y$ plane.

water on both ends of the channel was taken from a previous study.[51] The protein channel was aligned along the Z-axis. The lipid bilayer was then removed from the simulation box to save computation time.[51] To keep the protein structure near its initial configuration, all protein α carbons, except those which are within 6 Å of any of the embedded water molecules, were tethered with a force constant of 2.4 (kcal/mol)/Å^2 during the simulation. This way, the protein residues that have close contact with the water wire are allowed to reorganize during the proton transport process, while the tethered atoms fluctuate in a way similar to the full unconstrained simulation.[17,51]

For the classical hydronium case, a MTD trajectory was generated using the Z-coordinate of the hydronium oxygen atom as the reaction coordinate. Gaussian-shaped hills with H = 0.1 kcal/mol and w = 0.5 Å were added to the underlying potential surface every 500 steps. It is worth noting that in the combined MTD/US method the final PMF is not sensitive to the choice of these parameters, as long as they are in reasonable range,[24] since the PMF is not directly calculated from MTD. Soft walls were added on both ends at Z = 17 Å and Z = −20 Å, respectively, to limit sampling inside the channel. A 5 ns trajectory was generated, during which a "one-way" trip through the channel was made for the hydronium. Fifty snapshots were obtained from this trajectory at a 100 ps interval. These snapshots sampled diverse positions of the hydronium along the hydronium transport pathway. New MTD simulations were then initiated from each of these configurations to obtain better sampling of the pathway. For 32 of these MTD trajectories, at least one transport through the channel, from either direction, was observed within 3 ns. The transport part from each trajectory, the first one-way trip, was averaged to get the most possible hydronium transport pathway through the channel whereas other parts, which mainly sampled either end of the channel, were discarded. The path in each trajectory was found to be similar, indicating that no competitive pathways exist in this protein channel. For more complicated protein channels that do have more than one ion transport pathway having a similar free energy barrier, all pathways can be identified accordingly and the PMFs calculated separately.

A similar procedure was followed for the simulations with the excess proton treated using the MS-EVB model. In this case, the reaction coordinate is defined as the Z-coordinate of the center of the excess proton net positive charge defect (CEC), which is defined as[52]

$$\mathbf{r}_{\mathrm{CEC}} = \sum_{i}^{N_{\mathrm{EVB}}} c_i^2 \mathbf{r}_{\mathrm{COC}}^i \tag{4}$$

where c_i^2 is the EVB amplitude for state i and $\mathbf{r}_{\mathrm{COC}}{}^i$ is the center of charge vector

$$\mathbf{r}_{\mathrm{COC}}^i = \frac{1}{\mathrm{Q}_{\mathrm{tot.}}^i} \sum_{k}^{\{i\}} q_k \mathbf{r}_k \tag{5}$$

where

$$\mathrm{Q}_{\mathrm{tot.}}^i = \sum_{k}^{\{i\}} |q_k| \tag{6}$$

with q_k being the charge on atom k and $\mathbf{r}_k$ its position.

The averaged proton transport pathways through the channel are shown as yellow points for the classical hydronium model and blue points for the excess proton CEC in the MS-EVB model in the left panel of Figure 2. Both pathways are basically along the Z-coordinate but obviously deviate from a straight line. The right two panels of Figure 2 show that the pathways have excursions of more than 3 and 2 Å in the X- and Y-directions, respectively. (The projected pathways onto the $X-Y$ plane in these panels of Figure 2 would simply be dots in that plane if the pathways were straight lines along Z.) The MS-EVB model proton transport pathway is smoother than the classical hydronium model pathway, which is consistent with the fact that the MS-EVB model includes the Grotthuss mechanism of proton hopping explicitly so that multiple protons from different water molecules can

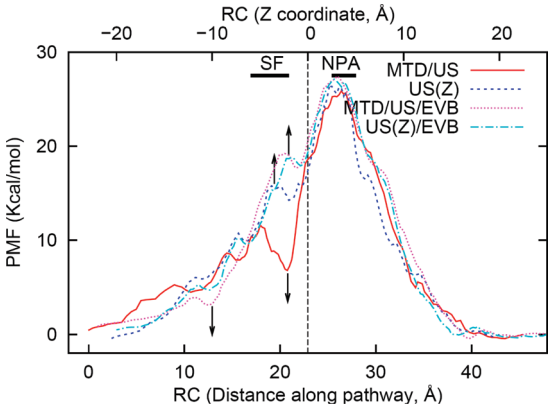

Figure 3. Free energy profile (or potential of mean force, PMF) calculated for the proton transport through the APQ1 channel using the *Z*-coordinate (up axis) or the displacement along the identified pathways (low axis) as the reaction coordinate, respectively. The proton was treated using either the classical hydronium model or the reactive MS-EVB model for the Grotthuss shuttling excess proton charge defect. The statistical error was estimated to be ±0.5 kcal/mol or smaller. The PMFs are aligned at Z = 0 Å as indicated by a dashed line. The position of NPA motif and the SF region was based on the *Z*-coordinate (upper axis).

participate in translocating the net positive excess proton charge defect.

It has been found previously that there are two barriers for proton transport through the AQP1 channel, corresponding to the selectivity filter region (SF, formed mainly by the Phe56, His180, and Arg195 residues) and the Asn-Pro-Ala (NPA) motifs.[16,45−51] The NPA motifs are shown in orange with the licorice helices model in Figure 2, and the SF region is in red. It is clear that the pathways are twisted in the $X-Y$ plane around the NPA motifs (red regions of the points in right panels of Figure 2), which was not directly noted before. While the proton transport pathways identified with different proton transport models seem similar for much of the channel, important differences are observed around the SF and NPA motif regions. Relative to the MS-EVB model case, the classical hydronium model pathway is repulsed further from the NPA motif residues, while the MS-EVB model appears to have the excess proton charge defect distorted further away from the center of the SF region.

The PMFs calculated using eq 2 along the MTD pathways and the ones calculated with the straight line *Z*-coordinate as the RC are shown in Figure 3. About 150 umbrella sampling windows are used for each case (0.25 Å interval for the channel region and 0.50 Å for the bulk region), and a constraining force constant of 30 (kcal/mol)/Å^2 was used. A 1 ns trajectory was generated for each window. The first 200 ps was considered equilibration and discarded when calculating the mean force using eq3. The dominant barrier due to the NPA motifs was found to be ∼27 kcal/mol for each case, similar to previous simulation results[51] of ∼28 kcal/mol using straight line RC with umbrella sampling and the weighted histogram analysis method. However, the smaller barrier at the selectivity filter region, as indicated in Figure 3, shows different features between the results. For the classical hydronium model simulations, when using the straight *Z*-coordinate as the RC, the barrier at SF is ∼16 kcal/mol, consistent with previous results[51] where the same RC was used, proving the accuracy of the mean force method used in this work. On the other hand, the barrier is only 11 kcal/mol when the PMF was calculated along the classical hydronium transport pathway identified by MTD. In addition, the minimum between the two barriers is significantly less deep when the *Z*-coordinate is used as the reaction coordinate. On the other hand, when the proton is treated using the MS-EVB model, the barrier at the SF region is ∼18−19 kcal/mol, which agrees well with previous MS-EVB results.[51] The two PMFs obtained with different RCs are different, but not as different as the classical hydronium model simulations.

In the calculations using the *Z*-coordinate as the RC, the system is free in the $X-Y$ plane. Previous studies found that the radius of the channel varies from more than 5 Å at the ends to less than 1 Å in the SF region.[45,51] In the simulation, the RC (*Z*-coordinate) windows were distributed evenly with a 0.25 Å interval; however, the actual distance between the sampled regions of two nearby windows can be much larger. Figure 4 shows the distance between the neighboring windows on the basis of the averaged position sampled in each window for the classical hydronium model case, in the *Z*-direction and absolute distance in 3D, respectively. In spite of a distance of less than 0.4 Å in the *Z*-direction, the absolute 3D distance between neighboring windows can be as large as 2.2 Å due to the distribution in the $X-Y$ plane. For pairs with the largest distance, the sampled region in the $X-Z$ and $Y-Z$ planes is shown in Figure 4. It is clear in the figure that the sampled regions are far away from each other in either the *X*- or *Y*-direction, despite good overlap in the *Z*-direction, causing a discontinuity in configurational space. It is obvious by comparing Figures 3 and 4 that the difference in the PMF is directly related to this discontinuity. The way the PMF is calculated in this work using eq 2 does not explicitly depend on the overlap between windows as it does in WHAM. However, such discontinuities introduce errors into the calculated PMF. When the proton hopping is described explicitly using the MS-EVB model, fewer bad overlap pairs were found (results not shown), but it still suffers from this problem when using the *Z*-coordinate as the RC.

The importance of a constraint in the direction perpendicular to the RC axis has been suggested before.[13] However, in the current PMF calculation using the *Z*-coordinate as the RC, no constraint was added for the proton in the $X-Y$ plane unless it is close to the bulk solvent (beyond Z = ±10.0 Å) because the equilibrium positions in the $X-Y$ plane for each umbrella sampling window in the channel region were not known explicitly. In addition, for a curved pathway, a constraint in the $X-Y$ plane perpendicular to the improperly chosen reaction coordinate along the *Z*-axis would cause errors as well, as demonstrated in the carbon nanotube model described earlier.

In the PMF calculation along the identified pathway described in the current work, a weak harmonic force of 5 (kcal/mol)/Å^2 was applied in the direction perpendicular to the normal of a given point on the pathway. As shown in Figure 4, the distance between neighboring windows are all reasonable (<1 Å). The fact that a weak force of 5 (kcal/mol)/Å^2 can constrain the system around the identified pathway highlights the reliability of the proposed combined MTD/US method.

IV. DISCUSSION AND CONCLUSIONS

A calculated ion permeation PMF is meaningful only if the reaction coordinate is correctly identified for the problem of interest. In the present work we have demonstrated using a simple artificial carbon tube model that a small kink or change in

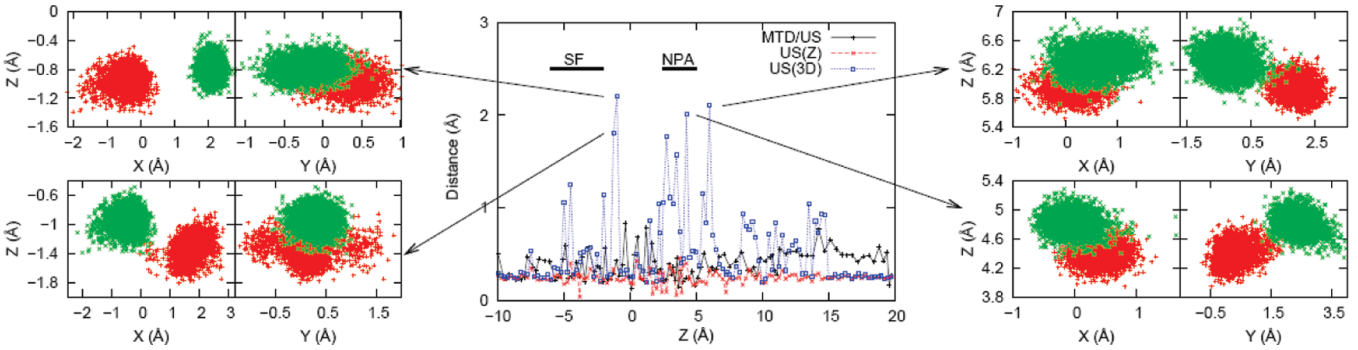

Figure 4. Distance between neighboring windows in the *Z*-direction (US(*Z*), dashed line) or in three dimensions (US(3D), dotted line) for the classical hydronium model simulation. The position for each window is calculated by taking the average of the sampled points, and only the pore part is shown. In the calculations using the *Z*-coordinate as the reaction coordinate, the RC is evenly distributed in the *Z*-direction with a 0.25 Å interval. However, the absolute distance between neighboring windows can be as large as 2.2 Å, causing discontinuities in the configuration space as shown for the four largest distance pairs. Such discontinuities introduce errors into the calculated PMF and may cause a misleading description of the ion permeation process. The simulation with the excess proton treated using the MS-EVB model suffers from a similar issue (not shown). The combined MTD/US (solid line) method avoids such problems.

channel radius can make an otherwise trivial calculation very complicated. The calculated PMF fully depends on the orientation of the tube, or in other words, it depends on the specific definition of the reaction coordinate.

Ion channel proteins help to establish the environment inside and outside of the cell by controlling the ion flow across the cell membrane. These heterogeneous pores are formed to perform various functions. Many of the ion channels are selective for some species over others by a specific gating mechanism. This feature makes the channel environment more complicated. For example, in AQP1, which conducts water but blocks all positively charged cation species, there are two gating motifs, the NPA motif and the SF region. Furthermore, the radius of the pore and the local environment varies greatly. As a result, the assumption of a straight ion transport pathway along a certain axis is highly questionable and introduces errors into the calculated PMF.

In the present study of AQP1, using the *Z*-coordinate as the RC overestimates the SF barrier by about 5 kcal/mol when the proton is treated using the classical hydronium model (cf. Figure 3). The NPA domain is still the dominant barrier region, and the barrier heights are similar when either RC definition was used. This is consistent with the fact that the channel radius at the SF region has a large variation from other parts of the channel,[45,51] highlighting the importance of a better definition of the RC in the PMF calculation. On the other hand, when the excess proton charge defect was treated using the MS-EVB model that allows proton (Grotthuss) shuttling, the PMFs obtained with both RC definitions are similar even in the SF region although small differences can be seen. This is due to the fact that the excess charge defect is delocalized over multiple waters in the MS-EVB model via the known proton hopping physics and results in a much smoother and continuous pathway as shown in Figure 2.

The results shown in Figure 3 for the AQP1 proton PMFs relative to those of the classical hydronium cation are, in fact, likely to be highly significant. This is because they support the notion that the APQ1 SF region is a specially evolved region of the channel designed to help block proton (shuttling H^+) flux (and it does so no matter what the chosen RC). On the other hand, the SF region it is not as important for blocking the flux by a "classical" hydronium cation that cannot shuttle protons (i.e., even though the "best" RC gives a small barrier for classical hydronium at the SF, a large barrier at the NPA region is still present). These ideas on the importance of the AQP1 SF region for modulating proton flux have recently been proposed from a combined computational/experimental study[54] of two AQP1 SF mutants, and the present results help to confirm this proposal.

It is further reasonable to anticipate that ion channel permeation studies for other ions (Na^+, Cl^-, etc) and proteins would also suffer the inaccuracies described earlier when an improper (e.g., straight line *Z*-coordinate) RC is used to calculate a PMF. The proposed combined MTD/US method however provides a computationally affordable and technically feasible solution to circumvent this problem.

In this work, we have used the MTD method to identify the ion transport pathway, but other pathway searching methods[55−63] could be used instead. For example, one such approach is the string method,[40,64] one version of which has been applied to biological systems by Roux and co-workers to study the conformational change of a small protein.[65] This method can also be applied to ion channel systems to identify the ion transport pathway that connects the two ends of the channel as well. However, the string method may not guarantee the identified pathway is the free energy minimum, which is the path most likely associated with the real processes in the cell. In MTD simulations, starting from one configuration, the system is more likely to cross the next lowest barrier and reach the other end of the channel along the free energy minimum pathway.

In the example described above, we have used the *Z*-coordinate as the RC in the MTD simulation, which is similar to an experimental setup where the ion concentration or an electrochemical gradient is applied in one direction to drive the ion flow. However, this is fundamentally different from the *Z*-coordinate RC used in normal umbrella sampling calculations. In the latter case, the simulation in each window is independent from the next window and can cause the discontinuity as observed above due to not enough sampling or other reasons. The MTD simulation, however, is a dynamical process and the successful transport through the channel guarantees continuous sampling. In addition, using the data from the first "one-way trip" assures the sampled path is the minimum corresponding to the most possible ion transport pathway observed in experiments.

The continuity of the sampled region can be further assured by applying a weak harmonic force in the perpendicular direction at a given point along the pathway when calculating the PMF.

In summary, the assumption that the ions transport through the nonuniform protein channel along a straight line can fail due to the complexity of the channel structure so that the PMF calculated along this path can be misleading. To get more reliable results, a combined MTD/US method has been proposed, in which the ion transport pathway is first identified using the MTD method. The PMF for the ion transport processes is then calculated along this pathway using the umbrella sampling method. This combined method also avoids the convergence problem sometimes found with the direct MTD approach for calculating a PMF. We have also applied the proposed method to the proton transport process through the AQP1 channel and demonstrated its feasibility, reliability, and ability to provide important new insight.

AUTHOR INFORMATION

Corresponding Author

*E-mail: gavoth@uchicago.edu.

Present Addresses

[†]Department of Chemical and Biomolecular Engineering, University of Notre Dame, Notre Dame, IN 46556.

ACKNOWLEDGMENT

This research was supported by the National Institutes of Health (Grant R01-GM53148). Computational resources were provided by the National Science Foundation through Teragrid computing resources administrated by the Texas Advanced Computing Center and the Pittsburgh Supercomputing Center, and by a grant of computer time from the Department of Defense High Performance Computing Modernization Program at the Maui High Performance Computing Center. We thank Dr. Takefumi Yamashita for helpful discussions.

REFERENCES

(1) Tajkhorshid, E.; Nollert, P.; Jensen, M. O.; Miercke, L. J. W.; O'Connell, J.; Stroud, R. M.; Schulten, K. *Science (Washington, DC, U. S.)* **2002**, *296*, 525.

(2) Dutzler, R.; Campbell, E. B.; MacKinnon, R. *Science (Washington, DC, U. S.)* **2003**, *300*, 108.

(3) Beitz, E.; Wu, B.; Holm, L. M.; Schultz, J. E.; Zeuthen, T. *Proc. Natl. Acad. Sci. U. S. A.* **2006**, *103*, 269.

(4) Wang, N.; Miller, C. *J. Mol. Biol.* **2006**, *362*, 682.

(5) Ho, J. D.; Yeh, R.; Sandstrom, A.; Chorny, I.; Harries, W. E. C.; Robbins, R. A.; Miercke, L. J. W.; Stroud, R. M. *Proc. Natl. Acad. Sci. U. S. A.* **2009**, *106*, 7437.

(6) Faraldo-Gomez, J. D.; Roux, B. *J. Mol. Biol.* **2004**, *339*, 981.

(7) Coleman, R. G.; Sharp, K. A. *Biophys. J.* **2009**, *96*, 632.

(8) Lin, Y.; Cao, Z.; Mo, Y. *J. Phys. Chem. B* **2009**, *113*, 4922.

(9) Phongphanphanee, S.; Yoshida, N.; Hirata, F. *J. Phys. Chem. B* **2010**, *114*, 7967.

(10) *Free Energy Calculations: Theory and Aplications in Chemistry and Biology*; Chipot, C.; Pohorille, A., Eds.; Springer: Berlin, Heidelberg, New York, 2007; Vol. 86.

(11) Burykin, A.; Warshel, A. *Biophys. J.* **2003**, *85*, 3696.

(12) Berneche, S.; Roux, B. *Proc. Natl. Acad. Sci. U. S. A.* **2003**, *100*, 8644.

(13) Allen, T. W.; Andersen, O. S.; Roux, B. *Proc. Natl. Acad. Sci. U.S.A.* **2004**, *101*, 117.

(14) Roux, B.; Allen, T.; Berneche, S.; Im, W. *Q. Rev. Biophys.* **2004**, *37*, 15.

(15) Allen, T. W.; Andersen, O. S.; Roux, B. *Biophys. J.* **2006**, *90*, 3447.

(16) Chen, H.; Wu, Y.; Voth, G. A. *Biophys. J.* **2007**, *93*, 3470.

(17) Wang, D.; Voth, G. A. *Biophys. J.* **2009**, *97*, 121.

(18) Dellago, C.; Hummer, G. *Phys. Rev. Lett.* **2006**, *97*, 245901.

(19) Hummer, G.; Rasaiah, J. C.; Noworyta, J. P. *Nature* **2001**, *414*, 188.

(20) Laio, A.; Parrinello, M. *Proc. Natl. Acad. Sci. U.S.A.* **2002**, *99*, 12562.

(21) Iannuzzi, M.; Laio, A.; Parrinello, M. *Phys. Rev. Lett.* **2003**, *90*, 2 38302/1.

(22) Ensing, B.; Vivo, M.; Liu, Z.; Moore, P.; Klein, M. L. *Acc. Chem. Res.* **2006**, *39*, 73.

(23) Bussi, G.; Laio, A.; Parrinello, M. *Phys. Rev. Lett.* **2006**, *96*, 090601.

(24) Laio, A.; Rodriguez-Fortea, A.; Gervasio, F. L.; Ceccarelli, M.; Parrinello, M. *J. Phys. Chem. B* **2005**, *109*, 6714.

(25) Gervasio, F. L.; Laio, A.; Parrinello, M. *J. Am. Chem. Soc.* **2005**, *127*, 2600.

(26) Gervasio, F. L.; Parrinello, M.; Ceccarelli, M.; Klein, M. L. *J. Mol. Biol.* **2006**, *361*, 390.

(27) Domene, C.; Klein, M. L.; Branduardi, D.; Gervasio, F. L.; Parrinello, M. *J. Am. Chem. Soc.* **2008**, *130*, 9474.

(28) Mantz, Y. A.; Branduardi, D.; Bussi, G.; Parrinello, M. *J. Phys. Chem. B* **2009**, *113*, 12521.

(29) Pfaendtner, J.; Dranduardi, D.; Parrinello, M.; Pollard, T. D.; Voth, G. A. *Proc. Natl. Acad. Sci. U. S. A.* **2009**, *106*, 12723.

(30) Barducci, A.; Bonomi, M.; Parrinello, M. *WIREs Comput. Mol. Sci.* **2011**, DOI: 10.1002/wcms.31.

(31) Micheletti, C.; Laio, A.; Parrinello, M. *Phys. Rev. Lett.* **2004**, *92*, 170601.

(32) Ensing, B.; Klein, M. L. *Proc. Natl. Acad. Sci. U. S. A.* **2005**, *102*, 6755.

(33) Wu, Y.; Schmitt, J. D.; Car, R. *J. Chem. Phys.* **2004**, *121*, 1193.

(34) Babin, V.; Roland, C.; Darden, T. A.; Sagui, C. *J. Chem. Phys.* **2006**, *125*, 204909.

(35) Min, D.; Liu, Y.; Carbone, I.; Yang, W. *J. Chem. Phys.* **2007**, *126*, 194104.

(36) Barducci, A.; Bussi, G.; Parrinello, M. *Phys. Rev. Lett.* **2008**, *100*, 020603.

(37) Nishihara, Y.; Hayashi, S.; Kato, S. *Chem. Phys. Lett.* **2008**, *464*, 220.

(38) Ceccarelli, M.; Anedda, R.; Casu, M.; Ruggerone, P. *Proteins: Struct., Funct., Bioinf.* **2008**, *71*, 1231.

(39) Kumar, S.; Bouzida, D.; Swendsen, R. H.; Kollman, P. A.; Rosenberg, J. M. *J. Comput. Chem.* **1992**, *13*, 1011.

(40) Maragliano, L.; Fischer, A.; Vanden-Eijnden, E.; Ciccotti, G. *J. Chem. Phys.* **2006**, *125*, 024106/1.

(41) Gan, W.; Yang, S.; Roux, B. *Biophys. J.* **2009**, *97*, L08.

(42) Smith, W.; Forester, T. R. The DL_POLY Molecular Simulation Package; http://www.dl.ac.uk/TCSC/Software/DL_POLY/main.html, Vol. *2009*, 1999.

(43) Cornell, W. D.; Cieplak, P.; Bayly, C. I.; Gould, I. R.; Merz, K. M., Jr.; Ferguson, D. M.; Spellmeyer, D. C.; Fox, T.; Caldwell, J. W.; Kollman, P. A. *J. Am. Chem. Soc.* **1995**, *117*, 5179.

(44) Bonomi, M.; Branduardi, D.; Bussi, G.; Camilloni, C.; Provasi, D.; Raiteri, P.; Donadio, D.; Marinelli, F.; Pietrucci, F.; Broglia, R. A.; Parrinello, M. *Comput. Phys. Commun.* **2009**, *180*, 1961.

(45) de Groot, B. L.; Grubmuller, H. *Science (Washington, DC, U. S.)* **2001**, *294*, 2353.

(46) de Groot, B. L.; Frigato, T.; Helms, V.; Grubmuller, H. *J. Mol. Biol.* **2003**, *333*, 279.

(47) Ilan, B.; Tajkhorshid, E.; Schulten, K.; Voth, G. A. *Proteins: Struct., Funct., Bioinf.* **2004**, *55*, 223.

(48) Chakrabarti, N.; Roux, B.; Pomes, R. *J. Mol. Biol.* **2004**, *343*, 493.

(49) Burykin, A.; Warshel, A. *FEBS Lett.* **2004**, *570*, 41.
(50) de Groot Bert, L.; Grubmuller, H. *Curr. Opin. Struct. Biol.* **2005**, *15*, 176.
(51) Chen, H.; Ilan, B.; Wu, Y.; Zhu, F.; Schulten, K.; Voth, G. A. *Biophys. J.* **2007**, *92*, 46.
(52) Day, T. J. F.; Soudackov, A. V.; Cuma, M.; Schmitt, U. W.; Voth, G. A. *J. Chem. Phys.* **2002**, *117*, 5839.
(53) Swanson, J. M. J.; Maupin, C. M.; Chen, H.; Petersen, M. K.; Xu, J.; Wu, Y.; Voth, G. A. *J. Phys. Chem. B* **2007**, *111*, 4300.
(54) Li, H.; Chen, H.; Steinbornn, C.; Wu, B.; Beitz, E.; Zeuthen, T.; Voth, G. A. *J. Mol. Biol.* **2011**, *407*, 607.
(55) Jonsson, H.; Mills, G.; Jacobsen, K. W. Nudged elastic band method for finding minimum energy paths of transitions. In *Classical and Quantum Dynamics in Condensed Phase Simulations*; Berne, B. J., Ciccotti, G., Coker, D. F., Eds.; World Scientific: Singapore, 1998; pp 385.
(56) Fischer, S.; Karplus, M. *Chem. Phys. Lett.* **1992**, *194*, 252.
(57) Henkelman, G.; Jonsson, H. *J. Chem. Phys.* **1999**, *111*, 7010.
(58) Isralewitz, B.; Gao, M.; Schulten, K. *Curr. Opin. Struct. Biol.* **2001**, *11*, 224.
(59) Bolhuis, P. G.; Chandler, D.; Dellago, C.; Geissler, P. L. *Annu. Rev. Phys. Chem.* **2002**, *53*, 291.
(60) Elber, R. *Curr. Opin. Struct. Biol.* **2005**, *15*, 151.
(61) van der Vaart, A.; Karplus, M. *J. Chem. Phys.* **2007**, *126*, 164106/1.
(62) Yang, H.; Wu, H.; Li, D.; Han, L.; Huo, S. *J. Chem. Theory Comput.* **2007**, *3*, 17.
(63) Zheng, L.; Chen, M.; Yang, W. *Proc. Natl. Acad. Sci. U. S. A.* **2008**, *105*, 20227.
(64) E, W.; Ren, W.; Vanden-Eijnden, E. *Phys. Rev. B: Condens. Matter Mater. Phys.* **2002**, *66*, 052301/1.
(65) Pan, A. C.; Sezer, D.; Roux, B. *J. Phys. Chem. B* **2008**, *112*, 3432.